

Retinal Vessel Segmentation Using Deep Neural Networks

Martina Melinscak^{1,2}, Pavle Prentasic² and Sven Loncaric²

¹Karlovac University of Applied Sciences, The University of Zagreb, J. J. Strossmayera 9, 47000 Karlovac, Croatia

²Faculty of Electrical Engineering and Computing, The University of Zagreb, Unska 3, 10000 Zagreb, Croatia
martina.melinscak@gmail.com, {pavle.prentasic, sven.loncaric}@fer.hr

Keywords: Blood vessel segmentation, retinal imaging, deep neural networks, GPU

Abstract: Automatic segmentation of blood vessels in fundus images is of great importance as eye diseases as well as some systemic diseases cause observable pathologic modifications. It is a binary classification problem: for each pixel we consider two possible classes (vessel or non-vessel). We use a GPU implementation of deep max-pooling convolutional neural networks to segment blood vessels. We test our method on publicly-available DRIVE dataset and our results demonstrate the high effectiveness of the deep learning approach. Our method achieves an average accuracy and AUC of 0.9466 and 0.9749, respectively.

1 INTRODUCTION

The retina is a layered tissue lining the inner surface of the eye. It converts incoming light to the action potential (neural signal) which is further processed in the visual centres of the brain. Retina is unique as blood vessels can be directly detected non-invasively in vivo (Abràmoff et al., 2010).

It is of great purpose in medicine to image the retina and develop algorithms for analysing those images. Recent technology in last twenty years leads to the development of digital retinal imaging systems (Patton et al., 2006).

The retinal vessels are connected and create a binary treelike structure but some background features may also have similar attributes to vessels (Fraz et al., 2012).

Several morphological features of retinal veins and arteries (e.g. diameter, length, branching angle, tortuosity) have diagnostic significance so can be used in monitoring the disease progression, treatment, and evaluation of various cardiovascular and ophthalmologic diseases (e.g. diabetes, hypertension, arteriosclerosis and choroidal neovascularization) (Kanski and Bowling, 2012; Ricci and Perfetti, 2007).

Because of the manual blood vessel segmentation is a time-consuming and repetitious task which requires training and skill, automatic segmentation of retinal vessels is the initial step in the develop-

ment of a computer-assisted diagnostic system for ophthalmic disorders (Fraz et al., 2012).

Automatic segmentation of the blood vessels in retinal images is important in the detection of a number of eye diseases because in some cases they affect vessel tree itself. In other cases (e.g. pathological lesions) the performance of automatic detection methods may be improved if blood vessel tree is excluded from the analysis. Consequently the automatic vessel segmentation forms a crucial component of any automated screening system (Niemeijer et al., 2004).

Conventional supervised methods are usually based on two phases: feature extraction and classification. Finding the best set of features (which minimizes segmentation error) is a difficult task as choice of features significantly affects segmentation. Recent works use convolutional neural networks (CNNs) to segment images so feature extraction itself is learned from data and not designed manually. These approaches obtain state-of-the-art results in many applications (Masci et al., 2013).

Where the idea for deep neural network (DNN) originated? Observing cat's visual cortex simple cells and complex cells were found. Simple cells are responsible for recognition orientation of edges. Complex cells show bigger spatial invariance than simple cells. That was inspiration for later DNN

architectures (Schmidhuber, 2014). DNNs are inspired by CNNs introduced in 1980 by Kunihiko Fukushima (Fukushima, 1980), improved in the 1990s especially by Yann LeCun, revised and simplified in the 2000s. Training huge nets requires months or even years on CPUs. In 2011, the first GPU-implementation (Ciresan et al., 2011a) of MPCNNs (max-pooling convolutional neural networks – MPCNNs) was described, extending earlier work on MPCNNs and on early GPU-based CNNs without max-pooling. GPU didn't make some fundamental enhancement in DNN, but faster training on bigger datasets allows getting better results in some reasonable time. A GPU implementation (Ciresan et al., 2011b) accelerates the training time by a factor of 50.

Our method is inspired by work of Ciresan et al. (2012) where they – in a similar problem of segmenting neuronal membranes in electron microscopy images – use deep neural network as a pixel classifier. They use the same approach in mitosis detection in breast cancer histology images which won the competition (IPAL, TRIBVN, Pitié-Salpêtrière Hospital, The Ohio State University n.d.).

The main contribution of this paper is demonstrating the high effectiveness of the deep learning approach to the segmentation of blood vessels in fundus images. We tested our results on publicly available dataset DRIVE (Staal et al., 2004).

The rest of the paper is organized as follows. In Related work we describe the state-of-the-art and give a brief overview of applied methods and their results. In section Methods we describe the proposed method of retinal blood vessel segmentation. Then follows a review of obtained results. In conclusion we give an overview of plans for future work which would lead to enhancements.

2 RELATED WORK

A large number of algorithms and techniques have been published relating to the segmentation of retinal blood vessels. These developments have been documented and described in a number of review papers (Bühler et al., 2004; Faust et al., 2012; Felkel et al., 2001; Fraz et al., 2012, 2012; Kirbas and Quek, 2004; Winder et al., 2009).

In this section we will give a brief overview of various methodologies. It is out of the scope of this paper to give detailed description of all algorithms and discuss advantages and disadvantages of all of them, but some current trends and discussion will be given to outline main problems and some future

directions. There are many works where algorithms were evaluated on the DRIVE database and, as we tested our methods on that database, it is illustrating to see previous results and which methods dominated and how much neural networks are represented.

A common categorization of algorithms for segmentation of vessel-like structures in medical images (Kirbas and Quek, 2004) includes image driven techniques (such as edge-based and region-based approaches), pattern recognition techniques, model-based approaches, tracking-based approaches and neural network based approaches. Similarly Fraz et al. (2012) in their overview divide techniques into six main categories: pattern recognition techniques, matched filtering, vessel tracking/tracing, mathematical morphology, multiscale approaches (Lindeberg, 1998; Magnier et al., 2014), model based approaches and parallel/hardware based approaches.

Many articles in which supervised methods are used have been published to date. The most prevalent approach in these articles has been matched filtering. The performance of algorithms based on supervised classification is better in general than on unsupervised. Almost all articles using supervised methods report AUCs of approximately 0.95. However, these methods do not work very well on the images with non uniform illumination as they produce false detection in some images on the border of the optic disc, hemorrhages and other types of pathologies that present strong contrast. Many improvements and modifications have been proposed since the introduction of the Gaussian matched filter. The matched filtering alone cannot handle vessel segmentation in pathological retinal images; therefore it is often employed in combination with other image processing techniques. Some results show that Gabor Wavelets are very useful in retinal image analysis. Also it can be seen that neural networks are not a very common approach (Fraz et al., 2012).

The problem in comparing experimental results could be in non uniform performance metrics which authors obtain for their results. Some papers describe the performance in terms of accuracy and area under receiver operating characteristic (ROC) whereas other articles choose sensitivity and specificity for reporting the performance.

In Fraz et al. survey (2012) algorithms achieve average accuracy in range of 0.8773 to 0.9597 and AUC from 0.8984 to 0.961. Detailed results can be seen in Fraz et al. (2012).

3 METHODS

We use a DNN, or more specifically convolutional neural networks (CNNs) which instead of subsampling or down-sampling layers have a max-pooling layer (MPCNNs).

MPCNNs consist of a sequence of convolutional (denoted C), max-pooling (denoted MP) and fully connected (denoted FC) layers. MPCNN can map input samples into output class probabilities using several hierarchical layers to extract features, and several fully connected layers to classify extracted features. During the training of the network, parameters of feature extraction and classification are jointly optimized (Ciresan et al., 2012).

Image processing layer (denoted I) is not required pre-processing layer. It is made of predefined non changeable filters.

2D filtering is applied between input images and a bank of filters in every C layer. It results with new set of images (denoted as maps). As in FC input-output representation maps are also linearly combined. After that, it is applied a nonlinear activation function (rectifying linear unit in our case).

In forward propagation if in front C layer is layer of size $n \times n$, we use $m \times m$ filter ω . Then size of C layer output is $(n - m + 1) \times (n - m + 1)$. The pre-nonlinearity input to some unit x_{ij}^l counts as:

$$x_{ij}^l = \sum_{a=0}^{m-1} \sum_{b=0}^{m-1} \omega_{ab} y_{(i+a)(j+b)}^{l-1} \quad (1)$$

Then nonlinearity is applied:

$$y_{ij}^l = \sigma(x_{ij}^l) \quad (2)$$

Table 1: 10-layer architecture for network. Layer type: I – input, C – convolutional, MP – max-pooling, FC – fully connected

Layer	Type	Maps and neurons	Filter size	Weights	Connections
0	I	1M x 65x65N	—	—	—
1	C	48Mx60x60N	6x6	1776	6393600
2	MP	48Mx30x30N	2x2	—	—
3	C	48Mx26x26N	5x5	57648	38970048
4	MP	48Mx13x13N	2x2	—	—
5	C	48Mx10x10N	4x4	36912	3691200
6	MP	48Mx5x5N	2x2	—	—
7	C	48Mx4x4N	2x2	9264	148224
8	MP	48Mx2x2N	2x2	—	—
9	FC	100N	1x1	19300	19300
10	FC	2N	1x1	202	202

Similarly to the method described in Ciresan et al. (2012), to train the classifier, we used all blood vessel pixels as positive examples, and the same

We follow closely the forward and back-propagation steps of MP layer which are in details described by Giusti et al (2013) and Masci et al (2013). MP layers are fixed and they are not trained. They take square blocks of C layers and reduce their output into a single feature. The selected feature is the most promising as max pooling is carried out over the C block. FC layers are the standard neural network layers where the output neurons are connected to all the input neurons, with each link having a weight as a parameter (Masci et al., 2013).

In order to do segmentation, image blocks are taken (with an odd number of pixels – the central pixel plus neighbourhood) to determine the class (vessel or non-vessel) of the central pixel. Network training is performed on patches extracted from a set of images for which a manual segmentation exists. After such training, the network can be used to classify each pixel in the new examples of images (Giusti et al., 2014).

After alternating four steps of C and MP layers two FC layers further combine the outputs into a 1D feature vector. The last layer is always a FC layer with one neuron per class (two in our case due to binary classification). In the output layer by using Softmax activation function each neuron’s output activation can be taken as the probability of a particular pixel.

In table 1 we show the 10-layer architecture for the network with numbers of maps and neurons, filter size for each layer, weights and connections for C and FC layers (Cireşan et al., 2013).

amount of pixels randomly sampled among all non blood vessel pixels. This ensures a balanced training set. The positive and negative samples are interleaved

ed when generating the training samples. We use the green channel of the input images as it is well known from the literature that the green channel contains the most contrast in fundus photographs. We do not preprocess the input images.

4 EXPERIMENTAL RESULTS

Training and testing of the proposed method was done using a computer with 2 Intel Xeon processors, 64 GB of RAM and a Tesla K20C graphics card. We decided to use the Caffe deep learning toolkit (Jia, Y. n.d.) in order to speed up the computation of parameters of the convolutional neural network. It takes approximately two days to train the network on the mentioned hardware.

We tested our method on publicly-available DRIVE dataset, which contains 40 images divided into a test and training set, both containing 20 images. An example for an original image and manual segmentation for the same image is shown in figure 1. Note that picture that shows manual segmentation is binary, but the output image is not, as outputs of the DNN are probabilities of each pixel to be a blood vessel. For practical purposes thresholding should be done to obtain a binary image.

In the retinal vessel segmentation process, the outcome is a pixel-based classification result. Notice that we do not rely on any bottom-up segmentation, since we treat semantic segmentation as pixel classification, where each pixel is described by its neighborhood. Therefore the method is not affected by the errors of bottom-up segmentation. In figure 1 we can see how a typical output image looks like. We can

see that areas belonging to blood vessels have higher probability of being part of blood vessels.

In order to quantitatively measure the performance of the proposed method we calculate the area under the ROC curve for each image, accuracy, true positive rate (TPR) and false positive rate (FPR). TPR represents the fraction of pixels correctly detected as vessel pixels while FPR is the fraction of pixels erroneously detected as vessel pixels. The accuracy is measured by the ratio of the total number of correctly classified pixels to the number of pixels in the image field of view. ROC curve plots the fraction of TPR versus FPR.

The method achieves an average accuracy of 0.9466 with 0.7276 and 0.0215 TPR and FPR, respectively on the DRIVE database. We obtained the threshold using the optimal operating point on the ROC curve, assuming the same costs of missclassifying both classes.

Average AUC is 0.9749, where minimal AUC is 0.9665 and maximal 0.9843. The ROC curves are calculated only for pixels inside the field of view of the image. In figure 2 and figure 3 we can see the original image, the softmax classification, and the ROC curve for the given image. In figure 2 AUC reach maximum and in figure 3 it is lowest. It can be seen that in the figure with the lowest AUC segmentation is much worse. That is due to pathologic modifications (there are some exudates seen on the original picture). In the DRIVE dataset there are not many fundus images with pathologic changes and probably it would be possible to suppress these false positives by including more pathologies in the training, however that would require annotations for pathologies and therefore such method would not be comparable to the published work. We leave this improvement for the future work.

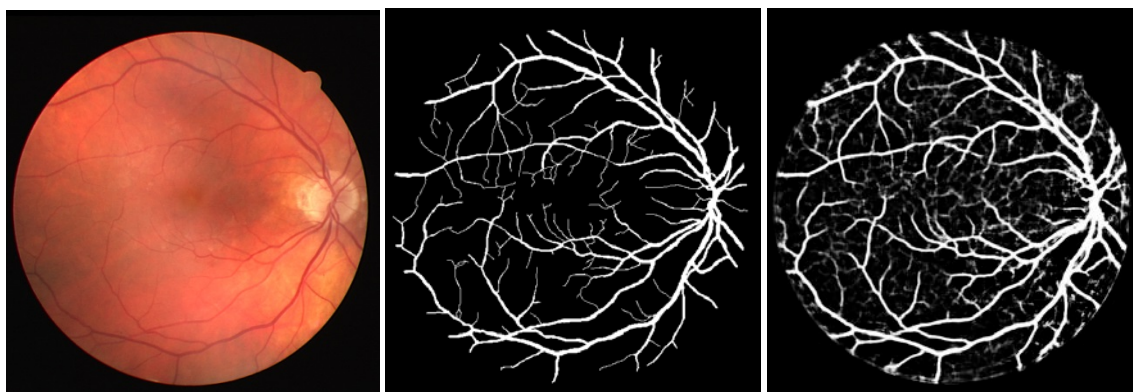


Figure 1: Retinal images from DRIVE. From left to right: original image, manual segmentation and output image.

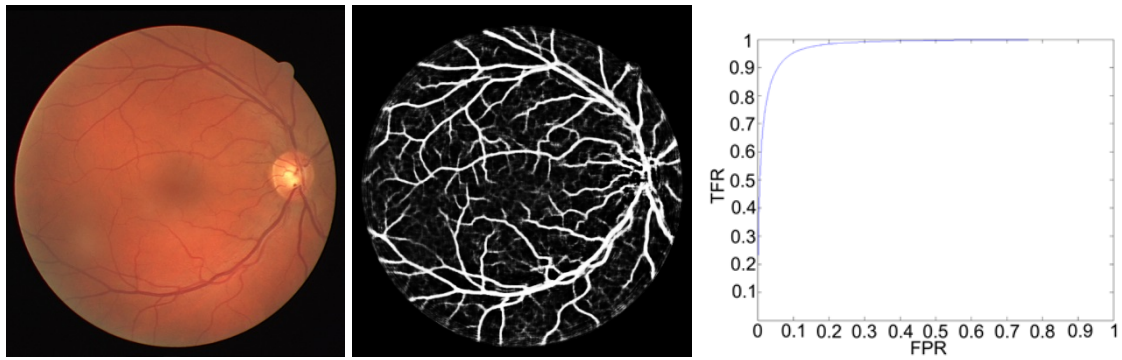


Figure 2: Original image, the softmax classification, and the ROC curve with maximum AUC (0.9843).

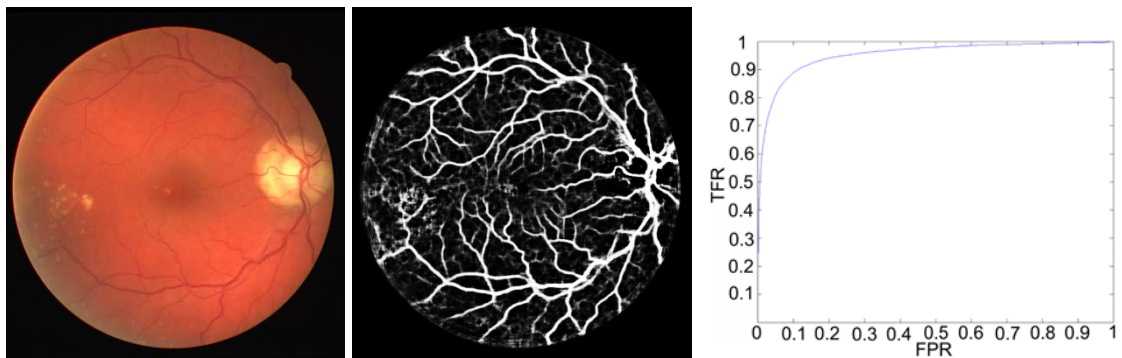


Figure 3: Original image, the softmax classification, and the ROC curve with lowest AUC (0.9665).

5 CONCLUSIONS

The segmentation of the blood vessels in the retina has been a heavily researched area in recent years. Although many techniques and algorithms have been developed, there is still room for further improvements.

We presented an approach using deep max-pooling convolutional neural networks with GPU implementation to segment blood vessels and results show that it is promising method. Our method yields the highest reported AUC for the DRIVE database, to the best of our knowledge.

In Fraz et al. survey (2012) algorithms achieve average accuracy in range of 0.8773 to 0.9597 and AUC from 0.8984 to 0.961. Our method achieves an average accuracy and AUC of 0.9466 and 0.9749, respectively. Minimal AUC is 0.9665 and maximal 0.9843.

Future work would be to enhance the algorithm by various methods like simulating more data for training: using all channels (not only green), to rotate, scale and mirror images etc. Perhaps some preprocessing and postprocessing would enhance

results and surely averaging more networks would improve results. Possibly foveation or non uniform sampling is also a way to enhance results. Training on a set with more images with pathologic changes might improve results.

There is also room for experimenting with non-linear activation functions to see whether they would improve results.

ACKNOWLEDGEMENTS

Authors would like to thank Josip Krapac for help with the definition and training of the neural network.

REFERENCES

- Abràmoff, M.D., Garvin, M.K., Sonka, M., 2010. Retinal Imaging and Image Analysis. *IEEE Rev. Biomed. Eng.* 3, 169–208. doi:10.1109/RBME.2010.2084567

- Bühler, K., Felkel, P., La Cruz, A., 2004. Geometric methods for vessel visualization and quantification—a survey. Springer.
- Caffe | Deep Learning Framework [WWW Document], n.d. URL <http://caffe.berkeleyvision.org/> (accessed 10.2.14).
- Cireşan, D.C., Giusti, A., Gambardella, L.M., Schmidhuber, J., 2013. Mitosis detection in breast cancer histology images with deep neural networks, in: *Medical Image Computing and Computer-Assisted Intervention—MICCAI 2013*. Springer, pp. 411–418.
- Ciresan, D.C., Meier, U., Masci, J., Maria Gambardella, L., Schmidhuber, J., 2011a. Flexible, high performance convolutional neural networks for image classification, in: *IJCAI Proceedings-International Joint Conference on Artificial Intelligence*. p. 1237.
- Ciresan, D.C., Meier, U., Masci, J., Maria Gambardella, L., Schmidhuber, J., 2011b. Flexible, high performance convolutional neural networks for image classification, in: *IJCAI Proceedings-International Joint Conference on Artificial Intelligence*. p. 1237.
- Ciresan, D., Meier, U., Schmidhuber, J., 2012. Multi-column deep neural networks for image classification, in: *Computer Vision and Pattern Recognition (CVPR), 2012 IEEE Conference on*. IEEE, pp. 3642–3649.
- Faust, O., Acharya, R., Ng, E.Y.-K., Ng, K.-H., Suri, J.S., 2012. Algorithms for the automated detection of diabetic retinopathy using digital fundus images: a review. *J. Med. Syst.* 36, 145–157.
- Felkel, P., Wegenkittl, R., Kanitsar, A., 2001. Vessel tracking in peripheral CTA datasets-an overview, in: *Computer Graphics, Spring Conference On, 2001*. IEEE, pp. 232–239.
- Fraz, M.M., Remagnino, P., Hoppe, A., Uyyanonvara, B., Rudnicka, A.R., Owen, C.G., Barman, S.A., 2012. Blood vessel segmentation methodologies in retinal images – A survey. *Comput. Methods Programs Biomed.* 108, 407–433. doi:10.1016/j.cmpb.2012.03.009
- Fukushima, K., 1980. Neocognitron: A self-organizing neural network model for a mechanism of pattern recognition unaffected by shift in position. *Biol. Cybern.* 36, 193–202.
- Giusti, A., Caccia, C., Ciresari, D.C., Schmidhuber, J., Gambardella, L.M., 2014. A comparison of algorithms and humans for mitosis detection, in: *Biomedical Imaging (ISBI), 2014 IEEE 11th International Symposium on*. IEEE, pp. 1360–1363.
- Image Sciences Institute: DRIVE: Digital Retinal Images for Vessel Extraction [WWW Document], n.d. URL <http://www.isi.uu.nl/Research/Databases/DRIVE/> (accessed 10.2.14).
- Kanski, J.J., Bowling, B., 2012. *Synopsis of Clinical Ophthalmology*. Elsevier Health Sciences.
- Kirbas, C., Quek, F., 2004. A review of vessel extraction techniques and algorithms. *ACM Comput. Surv. CSUR* 36, 81–121.
- Lindeberg, T., 1998. Edge detection and ridge detection with automatic scale selection. *Int. J. Comput. Vis.* 30, 117–156.
- Magnier, B., Aberkane, A., Borianne, P., Montesinos, P., Jourdan, C., 2014. Multi-scale crest line extraction based on half Gaussian kernels, in: *Acoustics, Speech and Signal Processing (ICASSP), 2014 IEEE International Conference on*. IEEE, pp. 5105–5109.
- Masci, J., Giusti, A., Cireşan, D., Fricout, G., Schmidhuber, J., 2013. A fast learning algorithm for image segmentation with max-pooling convolutional networks. *ArXiv Prepr. ArXiv13021690*.
- Mitosis Detection in Breast Cancer Histological Images | IPAL UMI CNRS - TRIBVN - Pitié-Salpêtrière Hospital - The Ohio State University [WWW Document], n.d. URL <http://ipal.cnrs.fr/ICPR2012/> (accessed 10.17.14).
- Niemeijer, M., Staal, J., van Ginneken, B., Loog, M., Abramoff, M.D., 2004. Comparative study of retinal vessel segmentation methods on a new publicly available database, in: *Medical Imaging 2004*. pp. 648–656.
- Patton, N., Aslam, T.M., MacGillivray, T., Deary, I.J., Dhillon, B., Eikelboom, R.H., Yogesan, K., Constable, I.J., 2006. Retinal image analysis: Concepts, applications and potential. *Prog. Retin. Eye Res.* 25, 99–127. doi:10.1016/j.preteyeres.2005.07.001
- Ricci, E., Perfetti, R., 2007. Retinal Blood Vessel Segmentation Using Line Operators and Support Vector Classification. *IEEE Trans. Med. Imaging* 26, 1357–1365. doi:10.1109/TMI.2007.898551
- Schmidhuber, J., 2014. Deep Learning in Neural Networks: An Overview. *ArXiv Prepr. ArXiv14047828*.
- Winder, R.J., Morrow, P.J., McRitchie, I.N., Bailie, J.R., Hart, P.M., 2009. Algorithms for digital image processing in diabetic retinopathy. *Comput. Med. Imaging Graph.* 33, 608–622.